The Role of Diabatic Heating, Torques and Stabilities in Forcing the Radial–Vertical Circulation within Cyclones Part III: Case Study of Lee–side Cyclones①

Donald R. Johnson and Zhuojian Yuan (袁卓建)

Space Science and Engineering Center, University of Wisconsin–Madison, Madison, WI 53706

(Received August 11, 1997)

ABSTRACT

Two phases of extratropical cyclone development identified in previous mass and angular momentum budget studies have been confirmed through the numerical simulations of the azimuthally–averaged mass–weighted radial motion within two leeside cyclones: a Mediterranean and an Alberta cyclone. In the Mediterranean cyclone, a moist baroclinic phase is identified with inward (outward) mass and storm angular momentum transport in the lower (higher) value isentropic layers. The mass and storm angular momentum are then transported diabatically from lower to higher value isentropic layers through latent heat release. In addition, storm angular momentum is transferred horizontally across the inclined isentropic surfaces by pressure stresses due to the paired negative and positive pressure torque in lower and higher value isentropic layers respectively. A dry–leeside baroclinic phase is identified in the early stage of the Alberta cyclone with inward (outward) transport of mass and angular momentum in the higher (lower) value isentropic layers. The redistribution of angular momentum is associated with the virtual transfer by torques. A transition from dry to moist phase is identified in the life cycle of the Alberta cyclone.

The present numerical results show that the dominant internal physical processes responsible for forcing the inflow and outflow within the Mediterranean cyclone are associated with pressure torque and horizontal eddy angular momentum transport, while within the Alberta cyclone the dominant internal processes are associated with inertial torque and pressure torque. The transfer of angular momentum from the higher value isentropic layer to the lower value isentropic layer is due to the virtual transfer by inertial torque in the dry phase of the Alberta cyclone. The transition from dry to moist phase within the Alberta cyclone results from the decrease of positive inertial torque and the intensification of negative pressure torque in the lower value isentropic layers.

Key words: Lee–side cyclone, Radial–vertical circulation

1. Introduction

An agreement between the simulated and "observed" azimuthally–averaged mass–weighted radial motions has been established for the Ohio cyclone and typhoon Nancy (Yuan and Johnson, 1998) with the use of the linear diagnostic equation derived in isentropic coordinates (Johnson and Yuan, 1998). In this isentropic numerical study, several physical processes which are not evident in isobaric studies are isolated. These processes include the effects of pressure torque, inertial torque and storm translation that are associated with the asymmetric structures in isentropic coordinates. Those processes explicitly described in both

①This research was sponsored by NASA Grant NAG 5–81.

isentropic and isobaric coordinates are also considered in this study as eddy angular momentum transport, diabatic heating and frictional torque. All these processes are modulated by static, inertial and baroclinic stabilities.

The results presented by Yuan (1997b) demonstrate the capability of the linear diagnostic equation to assess systematically the relative importance of the several physical processes in forcing the azimuthally-averaged mass-weighted radial-vertical circulation within extratropical and tropical cyclones. Now this capability is further tested in the study of the lee-side development of two cyclones. One cyclone occurred in the lee of the Alps Mountains (Mediterranean cyclone) in early March 1982. The other occurred in the lee of the Rocky Mountains (Alberta cyclone) in late March and early April 1971. Although both formed in spring and in the lee of mountains, previous mass and angular momentum budget studies (Johnson et al., 1976; Johnson and Hill, 1987; Katsfey, 1978; 1983) show that the patterns of "observed" radial mass and angular momentum transport within the Alberta cyclone are different from the patterns within the Mediterranean cyclone. Both moist and dry phases occur in the Alberta cyclone with the dry phase followed by the moist phase (Johnson et al., 1976; Katsfey, 1978; 1983), while only the moist phase occurs in the Mediterranean cyclone (Johnson and Hill, 1987). In the moist phase of development, import (export) of mass and angular momentum occurs in lower (higher) value isentropic layers, while for the dry phase import (export) occurs in the higher (lower) value isentropic layers. This study provides insight into the dominent internal physical processes responsible for forcing the inflow and outflow of the different phases and for the transition from dry to moist phase within the Alberta cyclone.

The numerical results and analyses for these two lee-side extratropical cyclones are presented in Section 2. A summary for this series of simulations involving the forcing of the radial-vertical circulation within three extratropical and one tropical cyclone is provided in Section 3.

2. Case study of two Lee-side cyclones

Previous investigations of cyclogenesis in the Northern Hemisphere (Petterssen, 1956; Whittaker and Horn, 1982) show that the highest frequency of extratropical cyclogenesis occurs in the lee of the mountains and over warm seas and ocean currents. Both orography and the warm Mediterranean sea are involved in the cyclone development in the lee of Alps, while only orography is involved in the development in the lee of Rockies. Thus, for this numerical study of lee-side development, the Mediterranean cyclone of 4-6 March 1982 and the Alberta cyclone of 30 March - 2 April 1971 are selected from a series of earlier mass and angular momentum budget studies of cyclone (Johnson and Downey, 1976; Wash, 1978; Katzfey, 1978; 1983; Hale, 1983; Rosinski, 1983; Schneider, 1986; Johnson, 1988; Johnson et al., 1976; Johnson, 1984; Johnson, and Hill, 1987; Hill, 1986).

2.1 *The Mediterranean cyclone of 4-6 March 1982*

2.1.1 *Synoptic situation*

At 0000 UTC 4 March 1982, a relatively intense 500 hPa trough orientated northeast-southwest approached the west coast of Europe from the Atlantic. The 500 hPa trough was associated with a strong surface cyclone centered over the North Sea. To the south of this strong surface cyclone, a weak surface low pressure disturbance could be identi-

fied over the east coast of Spain ahead of the 500 hPa deep trough.

By 1200 UTC 4 March, the 500 hPa trough had amplified as it moved over eastern Spain (Fig. 1d). The Alps and western Mediterranean Sea areas were under the influence of southwest flow ahead of the 500 hPa trough. At the surface to the northeast of the Balearic Island (Fig. 1a), a weak surface low pressure center (1016 hPa) was developing on a front extending southwestward from the Alps to the west of the Mediterranean Sea. The north–northwest flow to the west of the surface low with an embedded jet streak was stronger than the southwest flow to the east of the surface low. Precipitation occurred in France behind the cold front (Hill, 1986).

Twelve hours later at 0000 UTC 5 March, the 500 hPa trough split into two parts with the development of a cut-off low over the south coast of France (Fig. 1e). From the cut-off

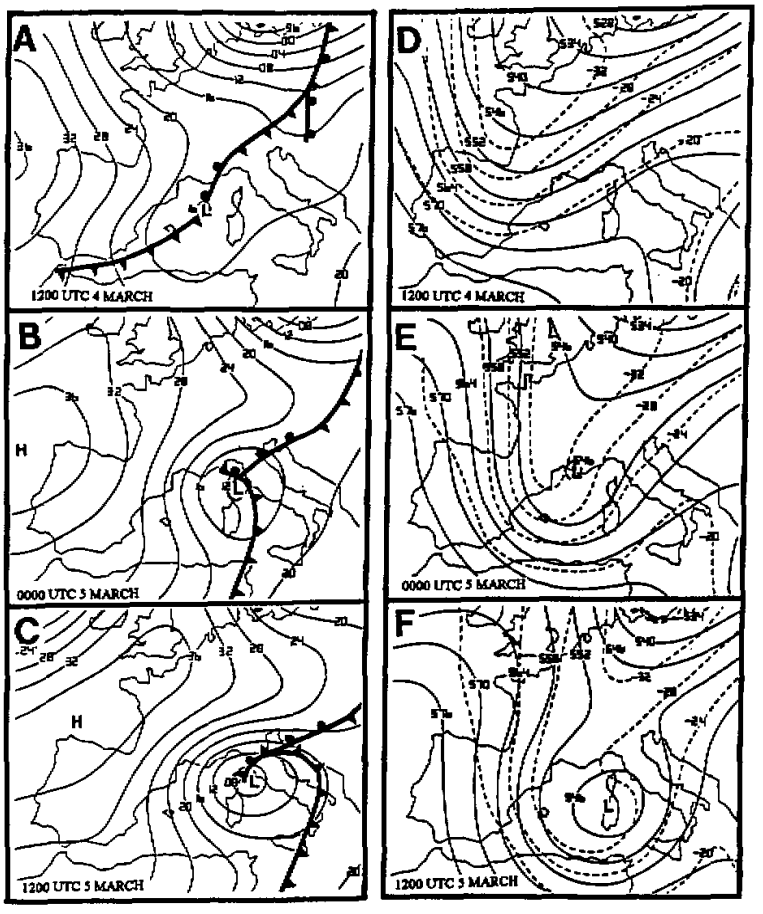

Fig. 1. Analyses of mean sea level pressure (hPa) (a)–(c) and 500 hPa height (dekameters, solid) and temperature (°C, dashed) (d)–(f) for the Mediterranean cyclone (Johnson and Hill, 1987).

low, the southern portion of the 500 hPa trough extended south-southwestward into the region over the western Mediterranean Sea. At the surface, the cold front had already moved southeast past the Alps (Fig. 1b). The surface low which initially formed near the Balearic Island deepened to 1011 hPa as it moved northeastward.

The lowest mean sea level pressure (MSLP) of 1006 hPa occurred at 0600 UTC 5 March (Hill, 1986) during its east-northeastward movement with an average speed of 3.3 m s^{-1} (Fig. 2). After 0600 UTC 5 March over the region between the Corsica Island and the west coast of Italy, the movement of the Mediterranean cyclone suddenly shifted towards the south and the cyclone started to fill. The occlusion of the cyclone was evident in the MSLP and 500 hPa analyses for 1200 UTC 5 March (Figs. 1c and f). The heaviest precipitation of 4 cm within a 12 hour period was observed at the surface in the northern portion of the cyclone (Hill, 1986). From 0000 UTC to 1800 UTC 6 March, the cyclone moved southeastward and decayed slowly.

2.1.2 *The data set*

Since the Mediterranean cyclone occurred during the Alpine Experiment (ALPEX), an assimilated ECMWF level IIIa data set with 6-hour interval prepared by ECMWF was available for diagnostic studies. The data set prepared by Johnson and Hill (1987) in their earlier mass and angular momentum budget study of the Mediterranean cyclone was used for this numerical study. In their isentropic analyses, the IIIa data set on standard isobaric surfaces was objectively interpolated to isentropic surfaces with a vertical resolution of 5 K. Then this data set was interpolated horizontally from the 1.875° lat / long grid to storm spherical coordinates (Johnson and Downey, 1975a).

2.1.3 *The forcing of radial-vertical circulation, the results and discussion*

In their earlier study of quasi-Lagrangian balance of mass and angular momentum within the Mediterranean cyclone of 4-6 March 1982, Johnson and Hill (1987) examined in detail the radial distribution of the geostrophic and ageostrophic components of the radial mass and

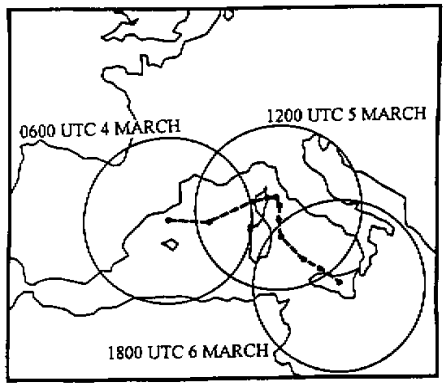

Fig. 2. Location of the 4.5° storm volume for the Mediterranean cyclone at six-hour interval from 0600 UTC 4 March to 1800 UTC 6 March 1982 (Johnson and Hill, 1987).

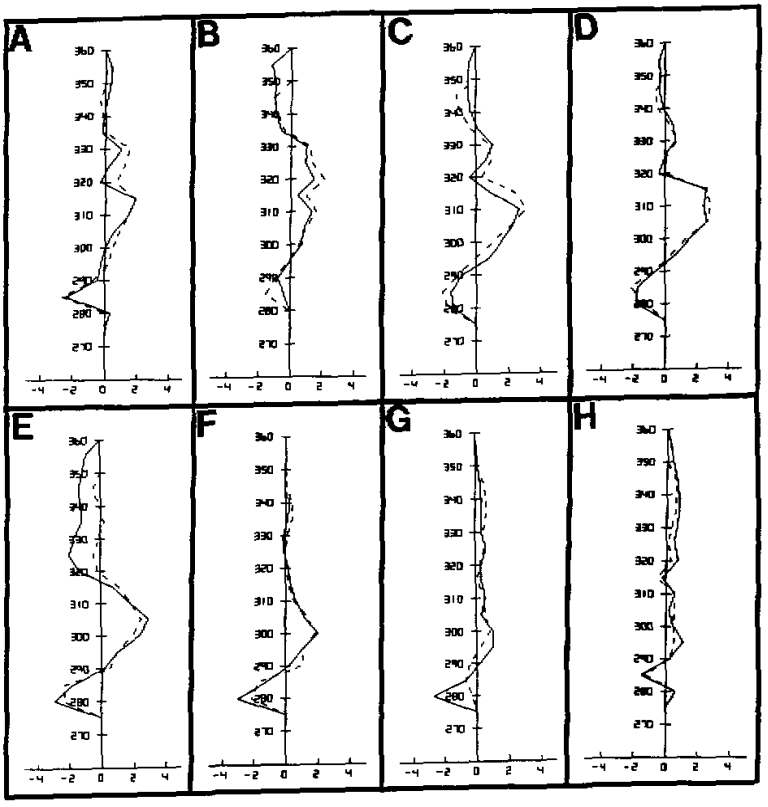

Fig. 3. Vertical profiles of simulated (dashed) and diagnosed (solid) azimuthally-averaged mass-weighted radial motion (m s^{-1} outflow positive) for the radius of 4.5° within the Mediterranean cyclone at (a) 1200 UTC 4, (b) 1800 UTC 4, (c) 0000 UTC 5, (d) 0600 UTC 5, (e) 1200 UTC 5, (f) 1800 UTC 5, (g) 0000 UTC 6 and (h) 0600 UTC 6 March 1982.

angular momentum transport. During the initial stage of cyclogensis, the geostrophic component, which is uniquely related to pressure torque, was dominant and increased with radius under the influence of the large-scale cold advection. Mass and angular momentum were carried into (out) the system by the geostrophic component of radial motion in the lower (higher) value isentropic layers. The combination of the net import of angular momentum and the effect of orography excited a self-development process in conjunction with the development of an S-shaped thermal wind pattern with inward eddy angular momentum transport in higher value isentropic layers. In the occlusion stage, inward angular momentum transport through the azimuthally-averaged mass-weighted radial motion was primarily forced by frictional torque and upward angular momentum transport through latent heat release. The following numerical results show the consistency with the early results.

In this isentropic study, the simulated azimuthally-averaged mass-weighted radial motions at radii equivalent to 1.5°, 3.0°, 4.5°, 6.0°, 7.5° and 9.0° latitudinal arcs are obtained numerically through solving the linear equation derived by Yuan (1997a) with open lateral

boundary conditions. The open lateral boundary conditions at the radius equivalent to 10.5° latitudinal arc are determined from quasi-Lagrangian diagnostic analysis (Yuan and Johnson, 1998). For the comparison with the previous mass and angular budget study (Johnson and Hill, 1987), the following analyses and discussion will focus on the numerical results for the radius equivalent to 4.5° latitudinal arc.

The simulated azimuthally-averaged mass-weighted radial motions for the radius of 4.5° (dashed profiles in Fig. 3) are in excellent agreement with the "observed" radial motions obtained from the quasi-Lagrangian diagnostic analysis of ECMWF level IIIa data (solid profiles in Fig. 3). The reason for the close agreement is that ECMWF provided a mutually consistent and relatively high temporal (6-hour) and spatial resolution data set for the diagnostic study of the Mediterranean cyclone. In Fig. 3 the dominant feature of the vertical distribution of azimuthally-averaged mass-weighted radial motion in isentropic coordinates is the maximum outflow above the maximum inflow. Both inflow and outflow reach their peak during the period between 0000 UTC 5 and 0000 UTC 6 March 1982 when strong baroclinic development occurs and an open wave amplifies. The moist development pattern is more pronounced for the larger radii with inward mass transport in the lower value isentropic layers and outward mass transport in the higher value isentropic layers (Fig. 4).

To gain initial insight into the relative importance of the various processes forcing the radial-vertical circulation within the Mediterranean cyclone, a preliminary comparison is carried out by inspecting the order of magnitude of forcing terms and hydrodynamic stability. Table 1 lists the maximum orders of magnitude of seven forcing terms along with the ranges of the order of magnitude of hydrodynamic stability at every time period for the radius of 4.5°. For the Mediterranean cyclone, the maximum magnitude of the forcing term associated with pressure torque (column 2) is one or two orders larger than those of other forcing terms in the early stage. Then with the development of axisymmetry, the maximum order of this forcing decreases to the same order as those of other forcing terms except for the term associated with the tilting of the angular momentum which is always the smallest.

In column 1 of Table 1, the maximum hydrodynamic stability at the first time period is one order of magnitude smaller than the rest. This is likely associated with the anticyclonic wind shear relative to isentropic surfaces at the first time period (Fig. 1d). Since for given forcing, the weaker hydrodynamic stability results in a stronger meridional circulation (Eliassen,

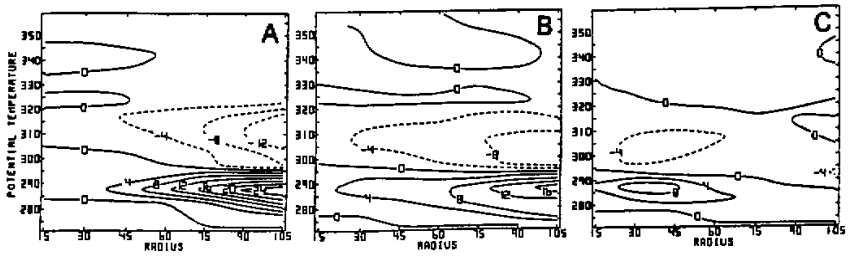

Fig. 4. Isentropic radial sections (to 10.5°) of azimuthally averaged radial mass transport (10^9 kg s^{-1}) within the Mediterranean cyclone for (a) 1200 UTC 4 March, (b) 0000 UTC March 5 and c) 1200 UTC 5 March 1982 (Johnson and Hill, 1987).

1951), the following discussion of the relative importance of different physical processes will include the effect of stability. This is accomplished by comparing the components of numerically simulated azimuthally-averaged mass-weighted radial motion in response to different internal forcing terms under closed outer boundary conditions. The following five subsections present the comparison among these results.

Table 1. The range of the magnitude of hydrodynamic stability and the maximum order of magnitude of forcing terms for the Mediterranean cyclone for the 4.5° radius

time	stability	term $1^{(1)}$	term $2^{(2)}$	term $3^{(3)}$	term $4^{(4)}$	term $5^{(5)}$	term $6^{(6)}$	term $7^{(7)}$
4^{12}	10^{-11}~$^{-12}$	10^{-11}	10^{-12}	10^{-12}	10^{-12}	10^{-12}	10^{-13}	10^{-13}
4^{18}	10^{-10}~$^{-12}$	10^{-11}	10^{-12}	10^{-12}	10^{-12}	10^{-12}	10^{-13}	10^{-13}
5^{00}	10^{-10}~$^{-12}$	10^{-11}	10^{-12}	10^{-12}	10^{-11}	10^{-12}	10^{-13}	10^{-12}
5^{06}	10^{-10}~$^{-12}$	10^{-11}	10^{-12}	10^{-12}	10^{-12}	10^{-12}	10^{-13}	10^{-11}
5^{12}	10^{-10}~$^{-12}$	10^{-11}	10^{-13}	10^{-12}	10^{-12}	10^{-12}	10^{-13}	10^{-11}
5^{18}	10^{-10}~$^{-12}$	10^{-12}	10^{-12}	10^{-12}	10^{-12}	10^{-12}	10^{-13}	10^{-12}
6^{00}	10^{-10}~$^{-12}$	10^{-12}	10^{-12}	10^{-12}	10^{-12}	10^{-12}	10^{-13}	10^{-12}
6^{06}	10^{-10}~$^{-12}$	10^{-12}	10^{-12}	10^{-12}	10^{-12}	10^{-12}	10^{-13}	10^{-12}

The unit of stability is $m^2\ s^{-4}\ hPa^{-2}$ and the unit of all the forcing term is $m\ s^{-3}\ hPa^{-1}$. The forcing terms associated with:

(1) pressure torque

(2) horizontal variation of azimuthally-averaged mass-weighted diabatic heating

(3) divergence of vertical eddy angular momentum transport

(4) divergence of horizontal eddy angular momentum transport

(5) inertial torque

(6) tilting of angular momentum towards or away from the local vertical axis due to cyclone's movement over the spherical earth

(7) frictional torque

(i) The effect of pressure torque

In the atmosphere where isentropic surfaces are above the earth's surface, the azimuthally-averaged mass-weighted pressure torque in isentropic coordinates can be alternatively expressed as an azimuthally averaged mode of geostrophic mass transport given by Johnson and Downey (1975b)

$$\overline{-\rho J_\theta \frac{\partial \psi}{\partial \alpha_\theta}} \Big/ \overline{\rho J_\theta} = \overline{\rho J_\theta f a \sin\beta (U_g)_\beta} \Big/ \overline{\rho J_\theta}, \tag{1}$$

where the Montgomery stream-function ψ is the sum of enthalpy c_pT and geopotential height gz. In lower atmosphere where isentropic surfaces intersect with the earth's surface, Lorenz's convention (Lorenz, 1955) is applied to the calculation of ψ. Following Lorenz's convention, the pressure and geopotential height on the "underground" isentropic surfaces ($\theta \leqslant \theta_S$, θ_S is the surface potential temperature) are set to their values at earth's surface respectively. Therefore, the effect of the orography is included in the azimuthally-averaged mass-weighted pressure torque within isenteropic layers that intersect the earth's surface (Johnson and Downey,

1975a, b; Johnson et al., 1976; Czarnetzki and Johnson, 1995).

The profiles of simulated azimuthally-averaged mass-weighted radial motion shown in Fig. 5 in isentropic coordinate for eight successive time periods are obtained from solving the linear equation with the only internal forcing associated with pressure torque. The relatively intense simulated radial motion from 1200 UTC 4 March to 0000 UTC 5 March (Figs. 5 a–d) coincides with the amplification of an open wave and the baroclinic development of a closed 500 hPa circulation (Fig. 1). After the cut-off circulation develops, the strength of the radial motions forced by pressure torque decreases due to the symmetric structure (Fig. 5 e–f). As expected, above the earth's surface, the distribution of simulated radial motion forced by pressure torque agrees with the distribution of the azimuthally integrated geostrophic component of lateral mass transport at the radius of 4.5° (Fig. 9c in Johnson and Hill, 1987).

As an example, the profile of the simulated azimuthally-averaged mass-weighted radial motion forced by pressure torque at 0000 UTC 5 March (Fig. 5c) is compared with the

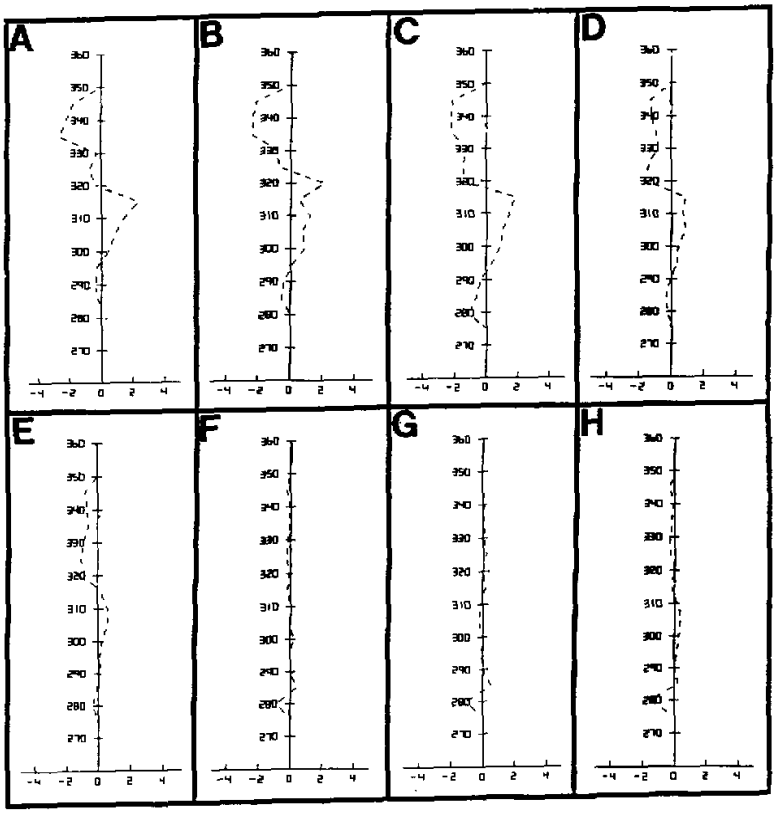

Fig. 5. Vertical profile of simulated azimuthally-averaged mass-weighted radial motion ($m\ s^{-1}$ outflow positive) forced by pressure torque for the radius of 4.5° within the Mediterranean cyclone at (a) 1200 UTC 4, (b) 1800 UTC 4, (c) 0000 UTC 5, (d) 0600 UTC 5, (e) 1200 UTC 5, (f) 1800 TUC 5, (g) 0000 UTC 6 and (h) 0600 UTC 6 March 1982.

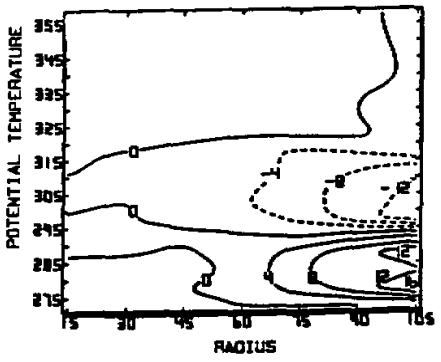

Fig. 6. Isentropic radial section (to 10.5 degrees) of geostrophic components of lateral mass transport (10^9 kg s^{-1} outward negative) within the Mediterranean cyclone at 0000 UTC 5 March 1982 (Johnson and Hill, 1987).

isentropic radial distribution of the geostrophic component of lateral mass transport at the same time (focus on the radius of 4.5° in Fig. 6) based on (1). Equation 1 indicates that above the earth's surface, the inward (outward) geostrophic component of lateral mass transport $[\rho J_\theta(U_g)_\beta$ less (greater) than zero] is associated with negative (positive) pressure torque. Therefore, the inward geostrophic component of lateral mass transport for the radius of 4.5° above 320 K (positive value in Fig. 6), which is in unison with the inward azimuthally-averaged mass-weighted radial motion (negative value above 320 K in Fig. 5c), is forced by negative pressure torque. Between 290 K and 320 K, the outward transport is forced by positive pressure torque.

Below 290 K with the influence of orography, the inward simulated azimuthally-averaged mass-weighted radial motion forced by pressure torque (Fig. 5c) is consistent with the results from several previous studies (Katzfey, 1978, 1983; Czarnetzky and Johnson, 1995), which show that in the lower atmosphere where isentropic surfaces intersect the mountain surface, pressure torque is negative (a sink of cyclonic angular momentum for the lower atmosphere). This sink of cyclonic angular momentum for the lower atmosphere is due to a stronger pressure gradient behind the cold front with more mass in isentropic layers to the north / northwest of the Mountains than the pressure gradient ahead of the cold front with less mass in isentropic layers to the south of the Mountains. This asymmetric distributions of pressure gradient force and mass around the low pressure center of a lee-side cyclone result in a sink of cyclonic angular momentum for the lower atmosphere through the cyclonic angular momentum transfer from the lower atmosphere to the earth across the inclined mountain surfaces. This is the exact case for the Mediterranean cyclone at 0000 UTC 5 March (Fig. 1c). A far more detailed discussion of pressure torque is given in the following study of the Alberta cyclone.

The results from the previous mass and angular momentum budget study of the Mediterranean cyclone (Johnson and Hill, 1987) show that 1) the geostrophic components of lateral mass transport (Fig. 6) and angular momentum transport increase in strength with the increase of radius in the early stage (Fig. 9 in Johnson and Hill) and 2) inward geostrophic

mass transport (related to negeative pressure torque) in lower value isentropic layers and outward geostrophic mass transport (related to positive pressure torque) in higher value isentropic layers are dominant at the larger radii. Concurrently, pressure stresses due to the paired positive and negative pressure torque lead to the non-convective transfer of storm absolute angular momentum from lower to higher value isentropic layers across inclined isentropic surfaces. These results indicate that the development of the Mediterranean cyclone in the early stage is associated with the large scale forcing associated with pressure torque.

(ii) The effect of horizontal eddy angular momentum transport

In their mass and angular momentum budget study of the Mediterranean cyclone, Johnson and Hill (1987) show that eddy angular momentum converges in higher value isentropic layers in the early stage of the development. As a source of angular momentum, the convergence of eddy angular momentum transport in higher value isentropic layers acts as a

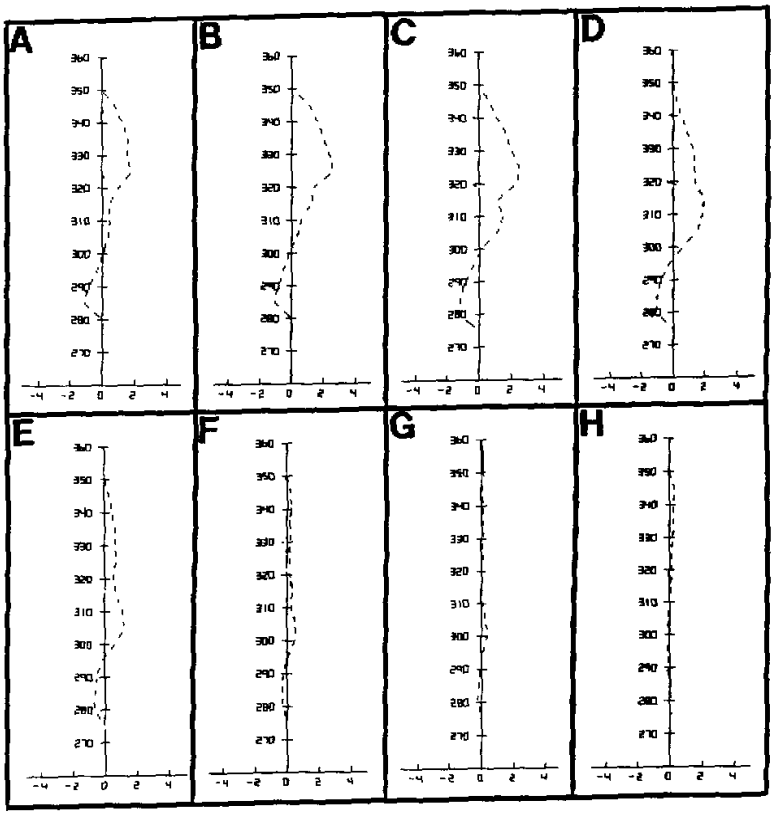

Fig. 7. Vertical profile of simulated azimuthally-averaged mass-weighted radial motion (m s^{-1} outflow positive) forced by horizontal eddy mode for the radius of 4.5° within the Mediterranean cyclone at (a) 1200 UTC 4, (b) 1800 UTC 4, (c) 0000 UTC 5, (d) 0600 UTC 5, (e) 1200 UTC 5, (f) 1800 UTC 5, (G) 0000 UTC 6 and (h) 0600 UTC 6 March 1982.

positive torque and forces outflow in these layers (Figs. 7a–e). The contribution of eddy mode to the forced radial motion is as large as pressure torque in the early stage. For example, at 0000 UTC 5 March, positive pressure torque forces a 1.5 m s^{-1} outflow at 310 K (Fig. 5c) and positive eddy mode also results in an outflow of 1.5 m s^{-1} at 310 K (Fig. 7c). Each of these accounts for half of the maximum total outflow of 3 m s^{-1} (dashed line in Fig. 3c). Above 320 K, the outflows (Figs. 7a–e) forced by positive eddy mode are partly canceled by the inflows (Figs. 5a–e) forced by negative pressure torque. Although the effect of eddy angular momentum transport on the radial motion decreases after 0600 UTC 5 March (Figs. 7d–h), the comparison of Figs. 5d and 7d shows that the process associated with eddy mode persists longer than that associated with pressure torque. This characteristic has also been noticed previously in the Ohio cyclone of 25–27 January 1978 (Yuan and Johnson, 1998).

The importance of the convergence of eddy angular momentum transport in the development of the Mediterranean cyclone has been emphasized by Johnson and Hill (1987). They pointed out that prior to 0000 UTC 5 March, the increase of the angular momentum in the higher value isentropic layers, in which the mean mode of angular momentum transport is outward, is due to the intense convergence of eddy angular momentum transport. As such, the excess of the convergence of eddy mode over the divergence of mean mode leads to the spin–up of the vortex in the higher value isentropic layers. The convergence of eddy angular momentum transport in the early stage of the Mediterranean cyclone is the combined effect of large scale baroclinic structure of environment, topographic forcing, thermal wind structure of fronts and corresponding upper–level jet streaks. As the large scale baroclinic wave approaches the west coast of Europe from the Atlantic, cold air blocked by the Alps Mountains flows through Rhone Valley into the Mediterranean to push the western portion of the front southward and enhance the cold front (Fig. 1). According to Johnson et al. (1976), Wash

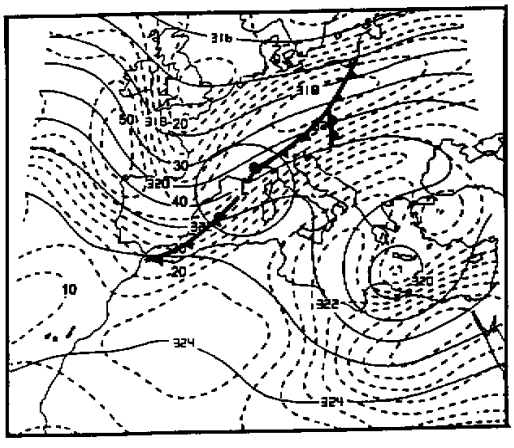

Fig. 8. Contours of Montgomery stream function (solid in 10^2 m^2 s^{-2}) and isotachs (dashed in m s^{-1}) for the Mediterranean cyclone on 325 K at 1200 UTC 4 March 1982. The circle with the radius equivalent to 4.5° latitudinal arc represents the position of the quasi–Lagrangian storm volume.

(1978) and Johnson and Hill (1987), an adjustment of upper-layer wind to the lower-layer baroclinic zone will take place through thermal wind. The thermal winds enhance the upper-level north-northwesterly jet to the west of France and the southwesterly jet over eastern Germany (Fig. 1a and Fig. 8). The storm volume, represented by the circle in Fig. 8, is located in the exit region on the cyclonic-wind-shear side of the north-northwesterly jet and in the entrance region on the anticyclonic-wind-shear side of the southwesterly jet. This is a favorable condition for the convergence of eddy angular momentum transport towards the storm's axis of rotation (Fig. 9e in Johnson and Hill, 1987; Johnson and Yuan, 1998; Yuan and Johnson, 1998).

(iii) The effect of diabatic heating

In isentropic coordinates, the vertical mass transport is directly associated with diabatic heating. From solving the continuity equation with the adjusted horizontal mass divergence (Johnson and Yuan, 1998), the azimuthally-averaged mass-weighted heating distributions for the radii of $\leqslant 4.5^{\circ}$ (Figs. 77, 78 in Yuan, 1994) are consistent with the mass-weighted area-averaged heating for a 4.5° storm volume (Fig. 5b in Johnson and Hill). Diabatic heating due to latent heat release increases in importance after 0600 UTC 5 March 1982 and contributes to upward absolute angular momentum transport and vertical development of cyclonic vortex. In the Mediterranean cyclone, the radial motion in response to the diabatic heating is small compared to those forced by pressure torque and horizontal eddy mode. This result is not shown here.

(iv) The effect of inertial torque

The azimuthally-averaged mass-weighted inertial torque stems from the acceleration / deceleration of the storm axis with respect to an absolute framework and asymmetric distribution of mass (Johnson and Downey, 1975b; Johnson and Yuan, 1998). Expanding this torque in a relative framework yields

$$\text{inertial torque} = -\langle \vec{l} \cdot \frac{d\overrightarrow{W_o}}{dt} \rangle a\sin\beta - \langle \vec{l} \cdot 2\vec{\Omega} \times \overrightarrow{W_o} \rangle$$
$$a\sin\beta + \langle \vec{l} \cdot \vec{\Omega} \times [\vec{\Omega} \times (\vec{r} - \overrightarrow{r_o})] \rangle a\sin\beta. \tag{2}$$

The first term of (2) deals with the acceleration / deceleration of the storm translation relative to the earth. The second term of (2) deals with the azimuthal component of Coriolis force due to the storm's relative velocity. Since the path of Mediterranean cyclone (Fig. 2) shows that during the life cycle of the Mediterranean cyclone, the direction of storm translation changes markedly from an eastward direction to a south-southeastward direction, the first term is as large as the second term. However, the combination of these two terms has a relatively small effect on the forcing of the radial motion (Figs. 80, 81 in Yuan, 1994). These results are not shown here. The third term is not discussed in this study since it is canceled by a corresponding forcing term associated with the tilting of storm angular momentum towards or away from the local vertical axis (Johnson and Yuan, 1998).

(v) The effect of frictional torque

As a sink of angular momentum, negative frictional torque forces inflow in the lower value isentropic layers of the Mediterranean cyclone (Figs. 82, 83 in Yuan, 1994). The forced inflow is weak in the early stage and then increases in strength due to the development of the

cyclonic circulation. Since the development of the cyclonic circulation is accompanied by the development of axial symmetry, the forcing of the radial motions through the baroclinic processes represented by pressure torque and eddy mode is suppressed as occlusion occurs. Therefore, the frictional torque becomes relatively important after 1200 UTC 5 and before 1800 UTC 5 March 1982 (Figs. 83a, b in Yuan, 1994). The same feature is described previously in the mass and angular momentum budget study of the Mediterranean cyclone (Fig. 22e in Hill, 1986).

2.1.4 *Summary*

In a previous quasi-Lagrangian mass and angular momentum budget study of the Mediterranean cyclone, Johnson and Hill (1987) concluded that the vertical structure of the azimuthally-averaged radial transport was characterized by the increasing strength of the inward (outward) geostrophic mass and angular momentum transport with radius in lower (higher) value isentropic layers. The intensification of the rotation in the lower troposphere due to the inward angular momentum transport in conjunction with the effect of topography excites the self-development process (Palmen and Newton, 1969). An upper-level S-shaped wind pattern associated with the self-development process favors the convergence of eddy angular momentum transport in the upper layers (Fig, 3 in Johnson and Hill, 1987). The convergence of angular momentum transport due to the geostrophic mode and eddy mode leads to the rapid development of the Mediterranean cyclone. In the late stage, inward mass and angular momentum transport by frictional torque and upward diabatic transport due to latent heat release become the relatively dominant factors.

The relatively important roles of pressure torque and eddy mode in the early stage and frictional torque and diabatic heating in the late stage of the Mediterranean cyclone are verified by the present numerical simulation of the forced azimuthally-averaged mass-weighted radial-vertical circulation by torques and diabatic heating. In the early stage, one of the dominant components of simulated radial motion is forced by pressure torque which is uniquely related to the geostrophic component of radial motion above the earth's surface. Another dominant component of simulated radial motion is associated with the eddy mode.

After the occlusion occurs at 1200 UTC 5 March, the cyclonic vortex becomes axially symmetric. With the symmetric structure, the effects of pressure torque and eddy mode on the forcing of the radial-vertical circulation decrease, while the effect of frictional torque increases. During this time period, the latent heat release associated with the significant precipitation becomes the important factor for the upward angular momentum transport.

2.2 *The Alberta cyclone of 30 March – 2 April 1979*

The Alberta cyclone of 30 March-2 April 1979 was selected for the purpose of ascertaining the similarities and differences in the development of cyclones in the lee of the Rockies over a land surface relative to the lee of Alps over the relatively warm Mediterranean sea. The development of the Alberta cyclone was one of the most interesting cases. Previous mass and angular momentum budget studies of the Alberta cyclone (Johnson et al., 1976; Katzfey, 1978; 1983; Holderbach, 1982) revealed a reversal of the azimuthally-averaged radial-vertical mass circulation during two different stages: a dry phase and a moist phase in the sense of negligible and extensive precipitation respectively. The present study will numerically investigate the relative importance of the processes responsible for the reversal of the radial-vertical circulation in isentropic coordinates.

2.2.1 *Synoptic situation*

At 1200 UTC 30 March 1971, the Alberta cyclone developed a 1002 hPa central MSLP in the lee of the Rockies to the north of Montana on a stationary polar front as a 500 hPa short wave trough approached the southwest coast of Canada (Figs. 9a, e). With the surface low being approximately located below a 500 hPa ridge, the relative phase between the 500 hPa trough and the surface low was about 180 degrees.

In the following 24 hours, the 500 hPa short trough moved east-southeastward with an axis located northeast-southwest over Idaho and Nevada (Fig. 9f). The amplitude of

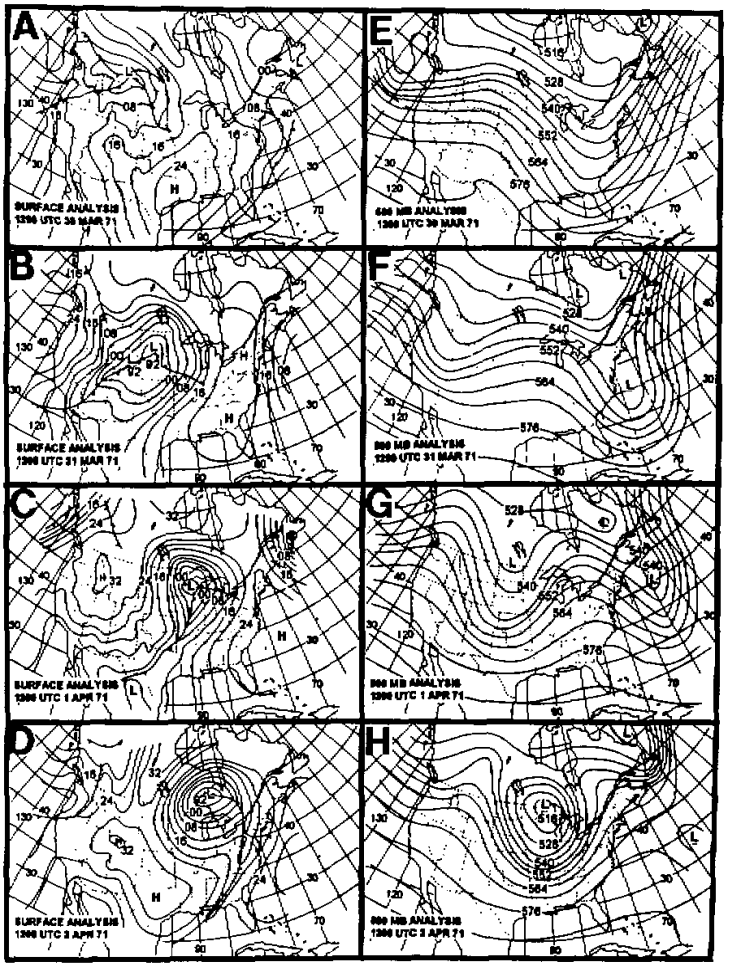

Fig. 9. Mean sea level pressure (hPa) (a)-(d) and 500 hPa heights (dekameters) analyses (e)-(h) for the Alberta cyclone (Johnson et al., 1976).

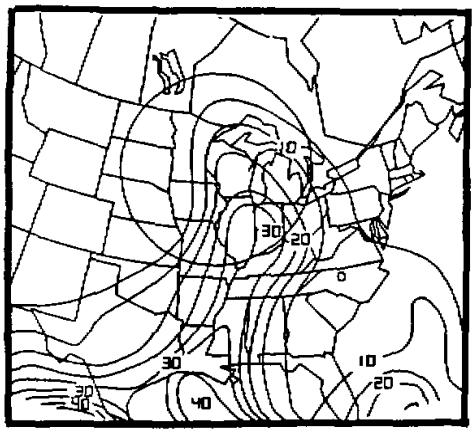

Fig. 10. Moisture distribution (10^{-1} g kg^{-1}) for the Alberta cyclone on 310 K at 1200 UTC 1 April 1971. The circle with the radius equivalent to 7.5° latitudinal arc represents the position of the quasi-Lagrangian storm volume.

the trough increased slightly during this time period. In the lower part of the atmosphere, the surface low was located in the north of the South Dakota and deepened to 990 hPa central MSLP by 1200 UTC 31 March (Fig. 9b). The main cold front was orientated southwestward from the low center and a quasi-stationary front extended east-southeastward from the low. During this 24-hour period, the phase difference between the 500 hPa trough and the surface low remained relatively constant. This indicated that the cyclone was still a shallow vortex with a warm core. Only very light precipitation was observed.

By 1200 UTC 1 April, the system changed direction and moved northeastward. The surface low was located in west central Wisconsin with central MSLP of 999 hPa (Fig. 9c). A moisture tongue intruded into the center of the system from the Gulf of Mexico (Fig. 10). Light precipitation was occurring to the northwest of the surface low. The 500 hPa trough, that was accompanied by a south-southwest-oriented jet streak with maximum wind speeds over 35 m s^{-1}, amplified significantly over the central United States (Fig. 9g). The phase between the 500 hPa trough and the surface low decreased markedly with cold air advection.

By 1200 UTC 2 April, a closed 500 hPa circulation developed over western Lake superior with the surface low being located slightly to the northeast of the 500 hPa cut-off low (Fig. 9d, h). Precipitation developed near the storm center with totals increasing markedly after 0600 UTC 1 April (Holderbach, 1982). Eventually, the circulation decayed as the surface and upper low slowly moved northeastward.

2.2.2 *The data set*

The data used for this study were prepared by Johnson et al. (1976) and Katzfey (1978) for the mass and angular momentum budget studies of the Alberta cyclone. The basic data set was the North American radiosonde observations with 12-hour interval. This data set was first interpolated vertically to prescribed isentropic levels with a vertical resolution of 5 K

(Johnson et al., 1976). Then the data were interpolated to 2 × 2 latitude–longitude grid by Cressman's method (Cressman, 1959). The final interpolation transferred all data to the storm spherical grid which consisted of seven concentric rings with radii equivalent to 1.5°, 3.0°, 4.5°, 6.0°, 7.5°, 9.0° and 10.5° latitudinal arc respectively with 36 grid points on each ring.

2.2.3 *The forcing of the radial–vertical circulation within the Alberta cyclone: results and discussion*

Johnson et al. (1976) and Katzfey (1978; 1983) have documented the mass and angular momentum budgets of the Alberta cyclone of 30 March–2 April 1971. In these isentropic studies two phases of development were identified within the life cycle of the Alberta cyclone. The first phase (dry phase) coincided with the strong warm advection over the Plains in the lee of the Rockies during an initial 48-hour development and was characterized by a azimuthally-averaged mass circulation with outward (inward) mass and angular momentum transport in the lower (higher) value isentropic layers. During the dry phase, the spin-up of the Alberta cyclone occurred due to the excess of the inward angular momentum transport in the higher value isentropic layers over the outward transport in the lower value isentropic layers. The second phase (moist phase), which occurred during the subsequent 48 hours, coincided with strong cold air advection and was characterized by a reversal of the mass circulation from that of the first phase. The azimuthally-averaged mass circulation of the moist phase was characterized by inward (outward) mass and angular momentum transport in the lower (higher) value isentropic layers. This inward mass and angular momentum transport in the lower value isentropic layers was associated with cold air advection. The cold air advection into the vortex led to the rapid advance of the 500 hPa trough relative to the surface circulation and the development of a cold core vortex. The occlusion resulted from the vertical redistribution of angular momentum by torques and diabatic heating.

The transition from dry to moist phase is associated with the change of forcing in isentropic coordinate. The present study is capable of providing insight into the physical processes responsible for this transition through the use of the linear equation derived by Yuan (1997a). This capability is ensured by the successful simulation of these two phases of radial–vertical circulation within the Alberta cyclone (Fig. 11). Fig. 11 shows the paired vertical profiles of azimuthally-averaged mass-weighted radial motion in isentropic coordinates for the Alberta cyclone. The dashed profile in each panel represents the simulated radial motion obtained from numerical solution of the linear diagnostic equation with open boundary conditions. The solid profile represents the "observed" radial motion obtained from the directly diagnostic analysis of the data used for this study. These profiles are in good agreement except for the relatively small differences for 0000 UTC 1 April (Fig. 11d). Notice that at 0000 UTC 1 April, the direction of movement of the Alberta cyclone changes from east-southeastward to east-northeastward (Fig. 12). This transition likely causes some difficulty in maintaining the consistency between the diagnosed and simulated radial motions due to the fact that temporal and spatial resolution of the radiosonde information is inadequate over this portion of the United States and Canada.

To investigate the processes responsible for the reversal of the radial–vertical circulation, the assessment of the relatively important forcing processes is now performed through a direct comparison among the maximum orders of magnitude of forcing terms (Table 2). Then the assessment is carried out through a comparison of the components of the simulated azimuthally-averaged mass-weighted radial motion obtained by solving the linear equation

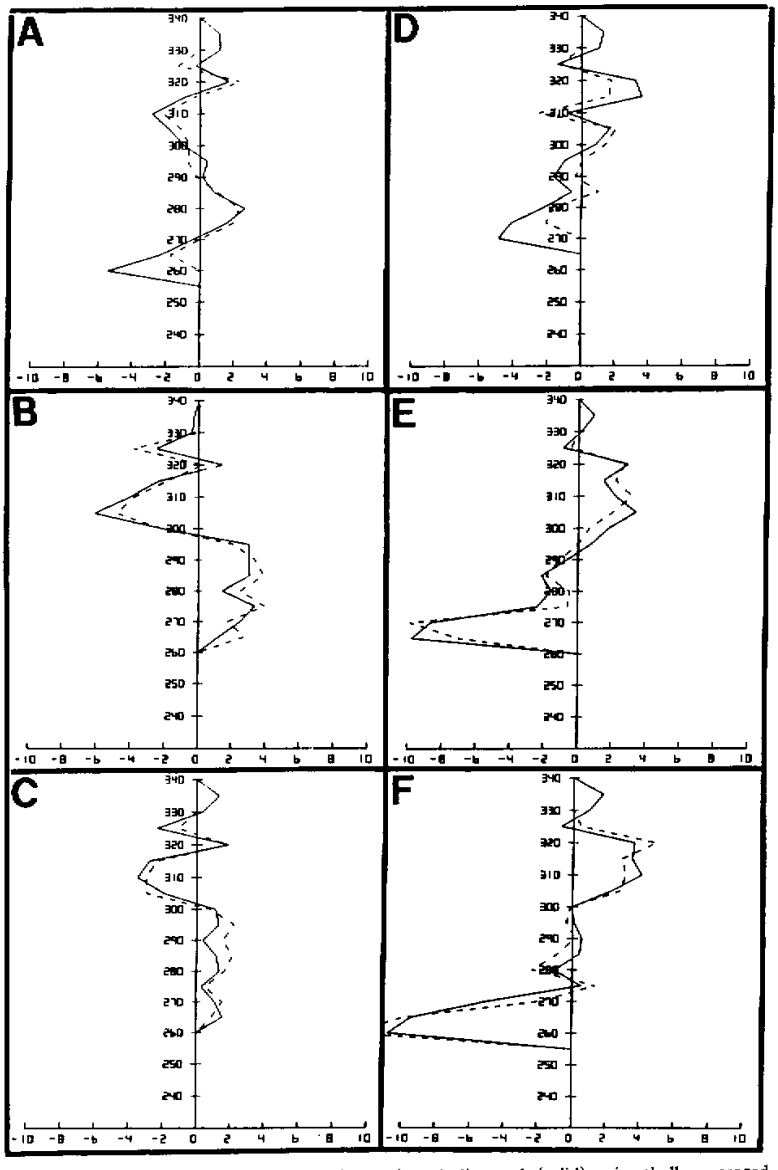

Fig. 11. Vertical profiles of simulated (dashed) and diagnosd (solid) azimuthally-averaged mass-weighted radial motion (m s^{-1} outflow positive) for the radius of 7.5° within the Alberta cyclone at (a) 1200 UTC 30, (b) 0000 TUC 31, (c) 1200 UTC 31 March, (d) 0000 UTC 1, (e) 1200 UTC 1 and (f) 0000 UTC 2 April 1971.

including only the internal individual forcing term with the influence of hydrodynamic stability.

Table 2 provides the direct comparison among the maximum orders of magnitude of

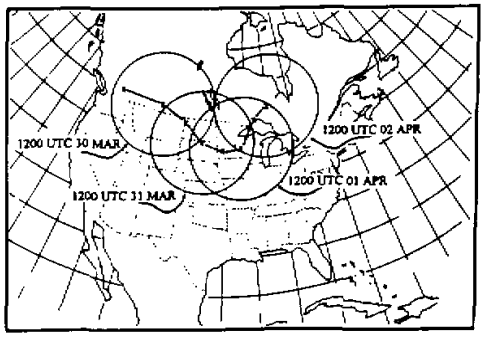

Fig. 12. Storm track and storm volumes of 7.5° equivalent latitudinal arc for the Alberta cyclone from 1200 UTC 30 March to 1200 UTC 2 April 1971 (Johnson et al., 1986).

Table 2. The range of the magnitude of hydrodynamic stability and the maximum order of magnitude of forcing terms for the Alberta cyclone for the 7.5° radius (See Table 1 for the meaning of each term)

time	stability	term $1^{(1)}$	term $2^{(2)}$	term $3^{(3)}$	term $4^{(4)}$	term $5^{(5)}$	term $6^{(6)}$	term $7^{(7)}$
30^{12}	$10^{-11}\sim-12$	10^{-11}	10^{-13}	10^{-12}	10^{-12}	10^{-11}	10^{-13}	10^{-13}
31^{00}	$10^{-11}\sim-12$	10^{-11}	10^{-12}	10^{-12}	10^{-12}	10^{-11}	10^{-13}	10^{-12}
31^{12}	$10^{-11}\sim-12$	10^{-11}	10^{-13}	10^{-12}	10^{-12}	10^{-11}	10^{-12}	10^{-12}
1^{00}	$10^{-11}\sim-12$	10^{-11}	10^{-13}	10^{-12}	10^{-12}	10^{-12}	10^{-13}	10^{-12}
1^{12}	$10^{-11}\sim-12$	10^{-11}	10^{-12}	10^{-12}	10^{-12}	10^{-11}	10^{-12}	10^{-12}
2^{00}	$10^{-11}\sim-12$	10^{-11}	10^{-12}	10^{-12}	10^{-11}	10^{-11}	10^{-12}	10^{-12}

seven forcing terms along with the ranges of the order of magnitude of hydrodynamic stability for every time period at the radius of 7.5°. Consistent with the results from previous studies (Johnson et al., 1976; Katzfey, 1978; 1983), the results shown in Table 2 indicate that the maximum magnitude of the forcing terms associated with pressure torque (column 2) and inertial torque (column 6) is one or two orders larger than those of other forcing terms. A comparison of Table 1 and Table 2 shows that the minimum magnitude of the hydrodynamic stability for the Alberta cyclone (column 1 in Table 2) is one order of magnitude smaller than that for the Mediterranean cyclone (column 1 in Table 1), while the strengths of forcing are the same. Therefore, according to Eliassen's perspective that for given forcing, the intensity of the radial–vertical circulation increases as the hydrodynamic stability decreases, stronger forced radial motions occur within the Alberta cyclone than within the Mediterranean cyclone (Figs. 3, 11).

To complete the investigation, the linear diagnostic equation, which includes the influence of the hydrodynamic stability on the forcing of the radial–vertical circulation by torques and diabatic heating, is used to simulate the component of the azimuthally–averaged mass–weighted radial motion corresponding to internal individual forcing under closed outer

boundary conditions. The results are presented in the subsection one to five followed by a brief summary.

(i) The effect of pressure torque

The azimuthally averaged mass-weighted pressure torque in isentropic coordinates can be expressed by (Johnson and Downey, 1975b)

$$-<\frac{\partial\psi}{\partial\alpha}>=-\overline{\rho J_\theta\frac{\partial\psi}{\partial\alpha}}\Big/\overline{\rho J_\theta}$$

$$=\{\frac{c_p\theta}{g(1+\kappa)p_{00}^{\kappa}}\overline{\frac{\partial}{\partial\alpha}(\frac{\partial}{\partial\theta}p^{1+\kappa})}+\frac{\partial}{\partial\theta}\overline{p\frac{\partial h}{\partial\alpha}}\}\Big/\overline{\rho J_\theta}, \tag{3}$$

where h represents the height of isentropic / earth surfaces and $\partial h/\partial\alpha$ is the slope of the isentropic / earth surface in the azimuthal direction. The first term in (3) involves the differences of the pressure stresses acting on the vertical-radial surfaces that are perpendicular to the azimuthal coordinate. With the use of Lorenz's convention (Lorenz, 1955; Johnson and Downey, 1975b), this term vanishes everywhere due to cyclic continuity in the azimuthal direction.

The second term stands for the component of pressure torque due to the differences of the azimuthal component of pressure stress vector $\vec{P}=p(\partial h/\partial\alpha)\vec{i}-p(\partial h/\partial\theta)\vec{k}$ acting on both upper and lower isentropic surfaces of an isentropic volume element (Katzfey, 1978, 1983; Czarnetzky and Johnson, 1995). Since the first term in (3) equals zero, the azimuthally averaged mass-weighted pressure torque becomes

$$-<\frac{\partial\psi}{\partial\alpha}>=\frac{\partial}{\partial\theta}\overline{(p\frac{\partial h}{\partial\alpha})}\Big/\overline{(\rho J_\theta)}. \tag{4}$$

Expression (4) states that mass-weighted azimuthally averaged pressure torque is associated with the derivative of the azimuthal component of pressure stress with respect to θ and serves as sources / sinks of cyclonic angular momentum within an isentropic layer due to the

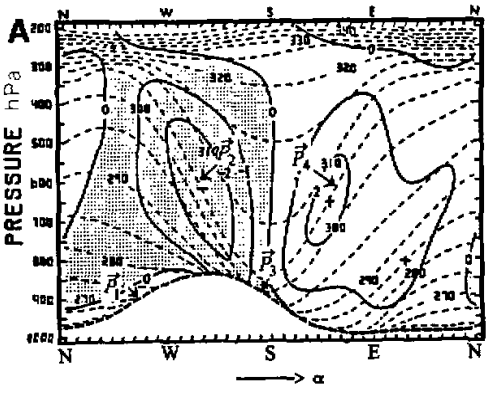

Fig. 13. Vertical-azimuthal distribution of azimuthal component of pressure stress on isentropic surfaces (solid) and potential temperature (dashed) for the radius of 9.0° within the Alberta cyclone at 1200 UTC 31 March 1971 (10^8 kg s^{-2}) (Katzfey, 1978). The cyclonic rotation (α) goes from the north (N) to the west (W), to the south (S), to the east (E) and back to the north.

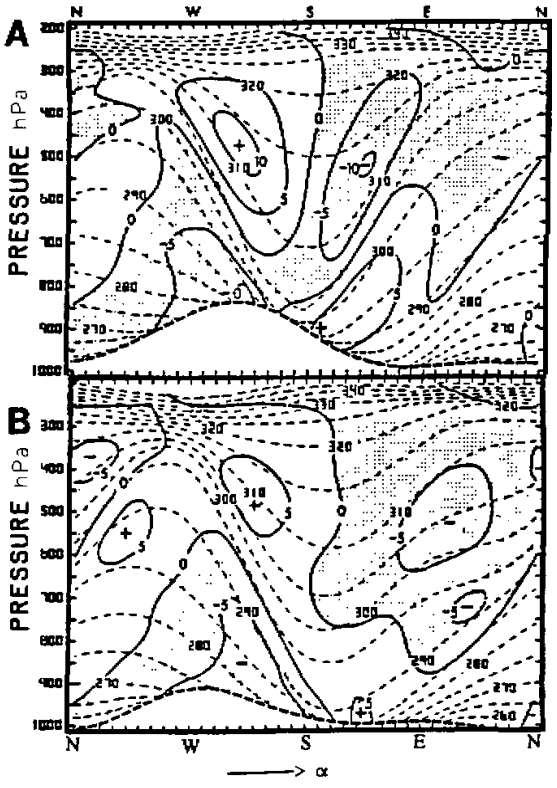

Fig. 14. Vertical-azimuthal distribution of vertical convergence pressure stress $\partial[p(\partial h / \partial x)] / \partial\theta$ (10^7 kg s^{-2}, solid) and potential temperature (K dashed) for the radius of 9.0° within the Alberta cyclone at (a) 1200 UTC 31 March and (b) 1200 UTC 1 April 1971 (Katzfey, 1978).

horizontal transfer across inclined isentropic / earth's surfaces. With the integration of (4) with respect to θ, this pressure torque reduces to the azimuthally integrated pressure stress at the earth's surface (Johnson and Downey, 1975b).

In a diagnostic study of momentum transfer by pressure stresses during the life cycle of a cyclone in the lee of the Rocky Mountains, Czarnetzki and Johnson (1995) point out that the mountain-induced negative pressure torque removes absolute dynamic circulation from the cyclone to the mountain (note that the vertically integrated tangential circulation on the boundary uniquely equals the vertically integrated absolute angular momentum weighted by the radius). The negative pressure torque results from the asymmetric distribution of pressure stresses due to a stronger pressure gradient to the northern portion than to the southern portion of the Rocky Mountains. Their result of mountain-induced neagative pressure torque is confirmed by this study of the Alberta cyclone in the lee-side of the Rocky Mountains.

The consistency between the distribution of pressure torque and the corresponding radial motion is now documented based on the present study and previous study of the Alberta cy-

clone by Katzfey (1978). Katzfey examined the pressure torque in detail for two different stages. The first stage is the dry leeside development stage (1200 UTC 31 March). Figure 13 shows the vertical–azimuthal distribution of the azimuthal component of pressure stress ($p\partial h / \partial \alpha$) of an upper domain on a lower domain (or the atmosphere on the mountains) across inclined isentropic (or mountain) surfaces for the radius equivalent to 9.0° latitudinal arc. Note that in Fig. 13 this azimuthal component of pressure stress is negative (positive) in the west (east) section with a center located along the cold (warm) front and the strongest $\vec{P}_2(\vec{P}_4)$ pointing towards the anticyclonic (cyclonic) direction due to the steepest negative (positive) slope of isentropic surface [$\partial h / \partial \alpha < 0 (\partial h / \partial \alpha > 0)$]. Fig. 13 also shows that the azimuthal component of pressure stress is positive (negative) in the northwest (southwest) section of the planetary boundary layer (PBL) with $\vec{P}_1(\vec{P}_3)$ pointing towards the cyclonic (anticyclonic) direction due to the positive (negative) slope of mountain surface. Thus, under the cold (warm) front in the western (eastern) section, this component of pressure torque , which is the derivative of the azimuthal component of pressure stress with respect to θ, serves as a sink (source) of cyclonic angular momentum for the lower atmosphere [negative (positive) pressure torque in Fig. 14a] due to $\vec{P}_2(\vec{P}_4)$ removes cyclonic angular momentum from the lower (upper) to the upper (lower) domain and $\vec{P}_1(\vec{P}_3)$ removes cyclonic angular momentum from the lower domain (the earth) to the earth (lower domain).

Katzfey's results (1978) and the present studies show that due to the stronger pressure gradient to the northern portion of the Rocky Mountains behind the cold front than to the southern portion of the Rocky Mountains ahead of the cold front (Fig. 9b, Fig. 13) at 1200 UTC 31, the azimuthally–averaged pressure torque is negative in the layers from 260 K to 290 K [focus on 1200 UTC 31 (3112) in Fig. 15] which forces inflow in this layer(Fig. 16a). The negative pressure torque around 310 K in Fig. 15 is associated with the steepest slope of the warm upper front (large $|\partial h / \partial \alpha|$) and the large amount of hydrostatic mass created by the stretching of isentropic layers as the storm moves away from the Rocky Mountains (Fig. 17a). The outflow around 300 K (Fig. 16a) is forced by positive torque (Fig. 15).

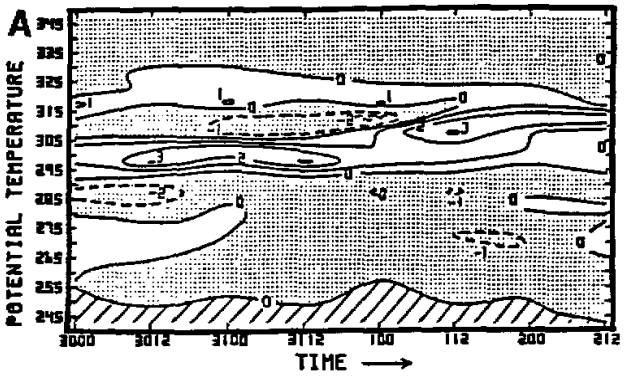

Fig. 15. Time variation of azimuthally averaged pressure torque (10^3 kg s^{-2}) for the Alberta cyclone from 0000 UTC 30 March to 1200 UTC April 1971 (Katzfey, 1978).

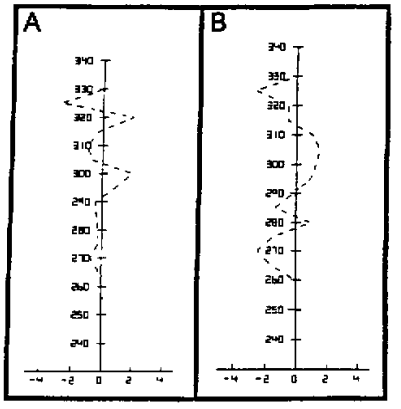

Fig. 16. Vertical profile of simulated azimuthally-averaged mass-weighted radial motion (m s $^{-1}$ outflow positive) forced by pressure torque for the radius of 9.0° within the Alberta cyclone at (a) 1200 UTC 31 March and (b) 1200 UTC 1 April 1971.

The following discussion will focus on the second stage: the moist development stage (1200 UTC 1 April). Fig. 15 shows that the negative azimuthally averaged pressure torque in the layer around 310 K at 1200 UTC 31 March becomes positive at 1200 UTC 1 April 1. To isolate the processes responsible for this change, the vertical-azimuthal distributions of hydrostatic mass (Fig. 17) and the pressure torque (Fig. 14) are compared for the dry and moist stages. The comparison of Fig. 14a with Fig. 14b shows that the magnitude of the negative values, centered around 310 K and associated with the positive slope of the upper warm front ($\partial h / \partial \alpha > 0$), has been reduced and shifted to the lower value isentropic layer. Obviously, these changes are associated with the decrease of the slope of upper warm front, the decrease of the intensity of the warm front (the reduced tightness of dashed lines in Fig. 14) and the decrease of hydrostatic mass around the upper warm front (Fig. 17). Corresponding to the positive pressure torque around 310 K at 1200 UTC 1 April (Fig. 15), the radial motion is now away from the center of the storm in the layer around 310 K (positive value in Fig. 16b).

(ii) The effect of inertial torque

For the Alberta cyclone, the inertial torque is mainly determined by term 2 in (2), which is associated with the azimuthal component of Coriolis force due to the relative velocity of the storm center. Since the azimuthal direction is counterclockwise, this component of inertial torque results in negative (positive) value [corresponding to storm relative inflow (outflow)] in the leading (trailing) half of the storm volume (Johnson and Yuan, 1998a). The radial motions forced by azimuthally-averaged mass-weighted inertial torque for the radius of 7.5° are shown in Fig. 19 for the dry stage (1200 UTC 31 March) and moist stage (1200 UTC 1 April). This component of radial motion represents the net storm relative mass transport due to the movement of the system in an asymmetric mass field.

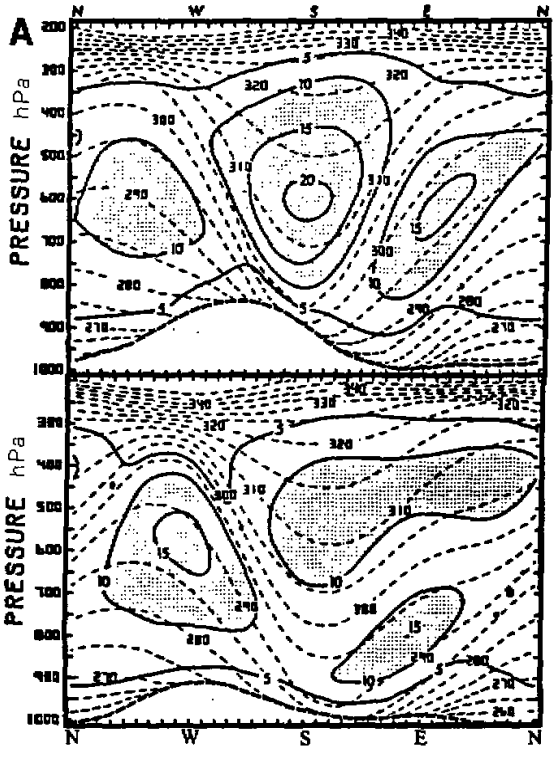

Fig. 17. Vertical–azimuthal distribution of hydrostatic mass (kg m^{-2}, solid) and potential temperature (K, dashed) for the radius of 9.0° within the Alberta cyclone at (a) 1200 UTC 31 March and (b) 1200 UTC 1 April 1971 (Katzfey, 1978).

At 1200 UTC 31 March 1971, the Alberta cyclone moved east–southeastward (Fig. 12) with negative (positive) inertial torque located in the east–southeastern (west–northwestern) half of the storm volume. The distribution of hydrostatic mass for an isentropic volume ($\rho J_\theta \Delta p / g$) at this time is non–axisymmetric around the Alberta cyclone (Figs. 20a–c) due to the Rocky Mountains and the confluence of maritime polar air masses and continental tropical air masses. Figure 20a illustrates that around 270 K more hydrostatic mass is located in the trailing half of the storm volume (with positive inertial torque) than in the leading half (with negative inertial torque). As a result, more mass moves into the system than out of the system due to the non–axisymmetric mass distribution and the existence of storm relative motion. In other words, the azimuthally–averaged mass–weighted inertial torque is positive in the layer around 270 K and forces an outflow (positive value in Fig. 19a). For the same reason, the outflow around 280 K in Fig. 19a is explained by more hydrostatic mass in the trailing half than in the leading half of the storm volume (Fig. 20b) in association with the cold dome to the north of the fronts (Katzfey, 1978). Up to 310 K, inflow shown in Fig. 19a is associated with more hydrostatic mass in the leading half of the storm volume (Fig. 20c) due to

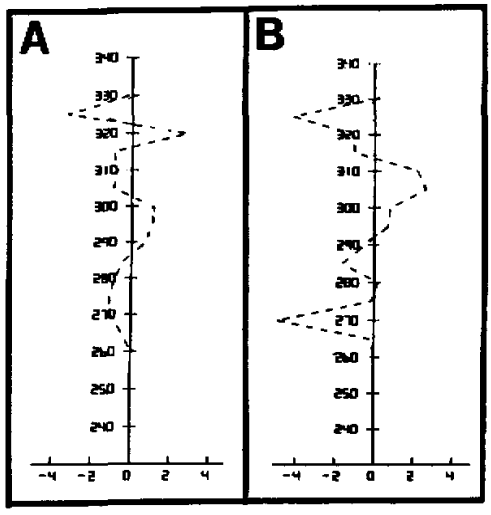

Fig. 18. Vertical profile of simulated azimuthally-averaged mass-weighted radial motion (m s $^{-1}$outflow positive) forced by pressure torque for the radius of 7.5° within the Alberta cyclone at (a) 1200 UTC 31 March and (b) 1200 UTC 1 April 1971.

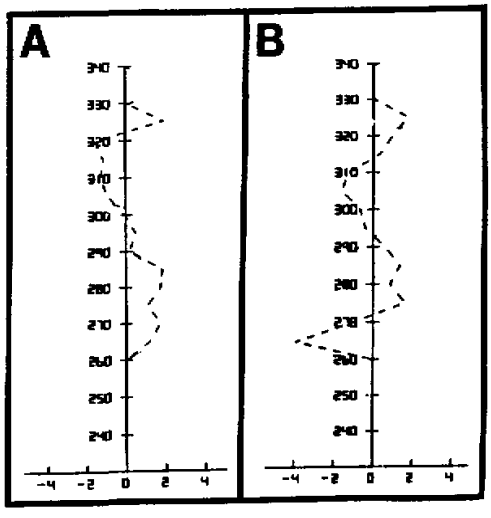

Fig. 19. Vertical profile of simulated azimuthally-averaged mass-weighted radial motion (m s $^{-1}$outflow positive) forced by inertial torque for the radius of 7.5° within the Alberta cyclone at (a) 1200 UTC 31 March and (b) 1200 UTC 1 April 1971.

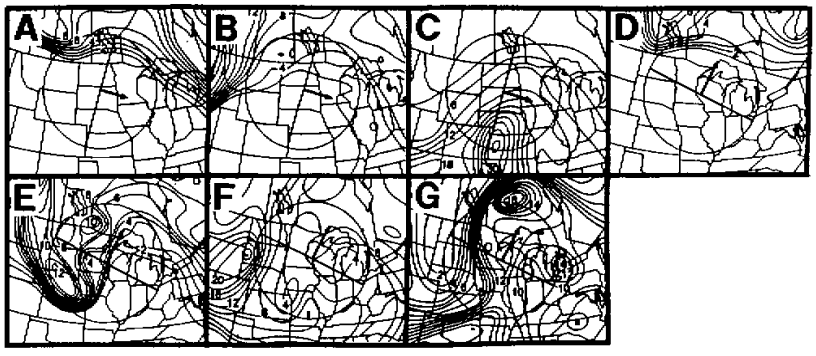

Fig. 20. Hydrostatic mass distribution (10^2 kg m $^{-2}$) for the Alberta cyclone on (a) 270 K, (b) 280 K, (c) 310 K isentropic surfaces at 1200 UTC 1 April 1971. The circle with the radius equivalent to 7.5° latitudinal arc represents the position of the quasi-Lagrangian storm volume.

the warmer air in the southern portion of the volume.

Different from the dry development, the moist development (1200 UTC 1 April 1971) is characterized by north-northeastward movement of the Alberta cyclone with negative (positive) inertial torque in the north-northeastern (south-southwestern) half of the storm volume (Fig. 12). Around 265 K (shown in Fig. 20d), the trailing half of the volume (with positive inertial torque) is totally under the ground (no hydrostatic mass in this half). Thus, the azimuthally-averaged mass-weighted inertial torque around 265 K is negative due to the fact that hydrostatic mass exists only in the leading half of the volume. The corresponding radial motion around this layer is toward the storm center (negative value in Fig. 19b).

Around 275 K and 285 K, the outflow in Fig. 19b is associated with more hydrostatic mass in the trailing half than in the leading half of the volume due to the penetration of cold air to the southwestern portion of the storm volume (Figs. 20e, f). The 305 K inflow results from the north-northeastward movement of the cyclone into a region with more hydrostatic mass (Fig. 20g).

A comparison of the distributions of radial motions forced by inertial torque and pressure torque (Figs. 19 and 18) reveals that the inertial torque is at least as important as pressure torque. For example, during the dry phase at 1200 UTC 31 March, the total outflow of 1.7 m s^{-1} at 280 K (Fig. 11c) is the sum of 1.8 m s^{-1} outflow due to positive inertial torque (Fig. 19a), 1 m s^{-1} inflow due to negative pressure torque (Fig. 18a) and 1 m s^{-1} outflow due to the effect of outer boundary condition. The latter is the homogeneous solution of the linear equation with open outer boundary conditions (Fig. 21a). During the moist phase at 270 K, the sum of the 2 m s^{-1} inflow forced by negative inertial torque (Fig. 19b), the 5.1 m s^{-1} inflow forced by negative pressure torque (Fig. 18b) and 2.3 m s^{-1} inflow in response to the outer boundary conditions (Fig. 21 b) accounts for most of the total inflow of 10 m s^{-1} (dashed line at 270 K in Fig. 11e). The transition from dry to moist development results mainly from the decrease of positive inertial torque in the lower value isentropic layers and the intensification of positive pressure torque in the higher value isentropic layers and negative pressure torque in the lower value isentropic layers.

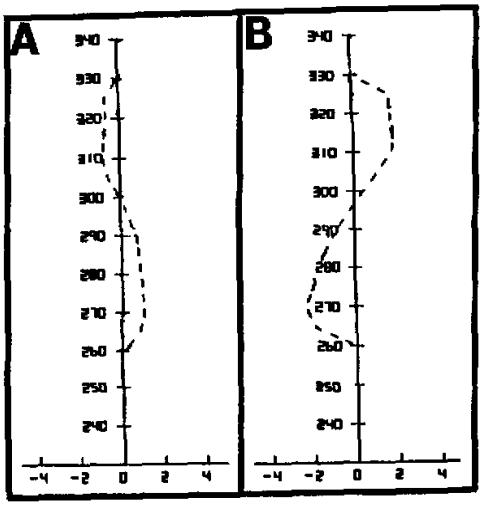

Fig. 21. Vertical profile of simulated azimuthally-averaged mass-weighted radial motion (m s^{-1} outflow positive) obtained from the numerical solution of the homogeneous equation with open outer boundary condition for the radius of 7.5° within the Alberta cyclone at (a) 1200 UTC 31 March and (b) 1200 UTC 1 April 1971.

(iii) The effect of vertical (diabatic) mass transport

In isentropic coordinates, the diabatic mass transport represents the vertical branch of radial-vertical mass circulation. The vertical-radial distribution of diabatic mass transport for the time periods from 1200 UTC 31 March to 1200 UTC April 2 1971 is shown in Fig. 22. In the leeside dry development with relative cloud free condition (Figs. 22 a, b), the upward diabatic mass transport is minimal. After 1200 UTC April 1, the upward diabatic mass transport due to latent heat release gradually intensifies (Figs. 22c, d). According to Johnson et al. (1976), the upward diabatic angular momentum transport through latent heat release combined with the increase of transfer of angular momentum across inclined isentropic surfaces by inertial and pressure torques in the moist development stage leads to the occlusion of the Alberta cyclone.

(iv) The effect of horizontal eddy mode

In a previous study, Johnson et al. (1976) point out that at 0000 UTC 31 March, areally integrated eddy angular momentum transport in the layer around 305 K is divergent [negative value at 0000 UTC 31 (3100) in Fig. 23]. This divergence of eddy angular momentum transport constitutes a momentum sink (negative horizontal eddy mode) for the Alberta cyclone. At 0000 UTC April 2 the eddy angular momentum transport in the layer around 305 K becomes convergent (positive value in Fig. 23), which constitutes a momentum source (positive horizontal eddy mode) for the system.

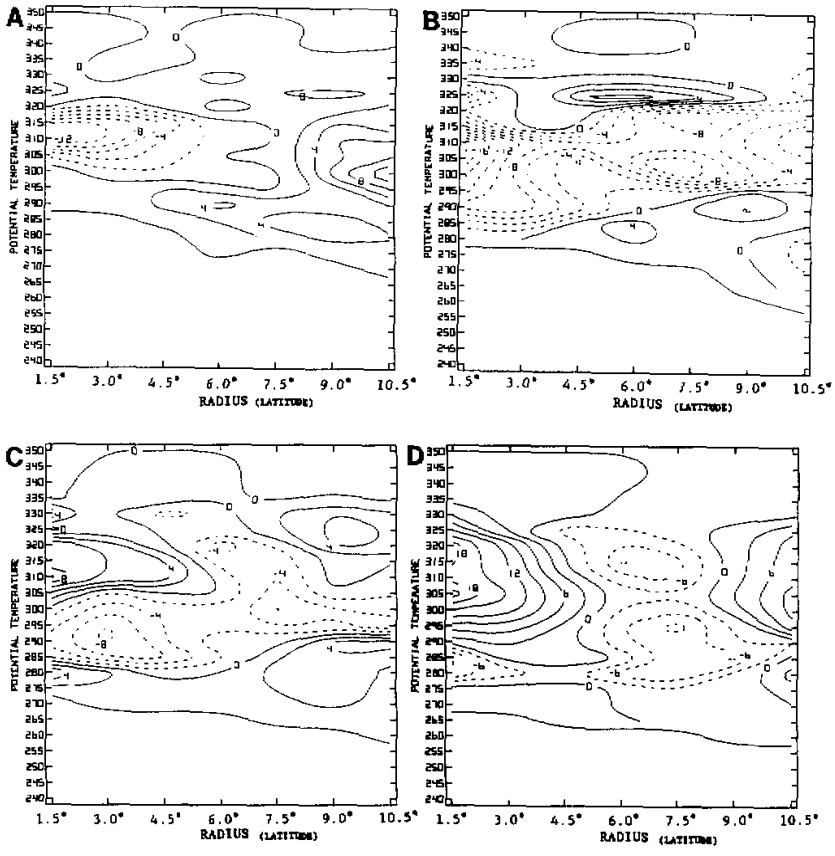

Fig. 22. Vertical–radial distribution of vertical (diabatic) mass transport per unit area (10^{-3} kg s^{-1} m^{-2}) for the Alberta cyclone for (a) 1200 UTC 31 March–0000 UTC 1 April, (b) 0000 UTC–1200 UTC 1, (c) 1200 UTC–0000 UTC 2 and (d) 0000–1200 UTC 2 April 1971.

From the forcing of the radial–vertical circulation point of view, the negative (positive) horizontal eddy mode, acting like a torque, will force inward (outward) radial motion within cyclones. Thus the negative eddy mode around 305 K at 0000 UTC 31 March (Fig. 23) is responsible for the inflow around 305 K (negative value in Fig. 24a). This net inflow forced by the negative horizontal eddy mode is consistent with the synoptic situation (Fig. 25a). Figure 25a shows that at 0000 UTC 31 the vortex volume is located in the convergence area which is on the anticyclonic shear side in the exit region of a jet streak. As the Alberta cyclone moves away from the Rocky Mountains and interacts with the moist air from the Gulf of Mexico, the phase difference between the trough in the upper isentropic surface and the surface low decreases. Within this time period the transition from dry to moist development occurs. During moist baroclinic development, the adjustment of upper-level wind to the low-level

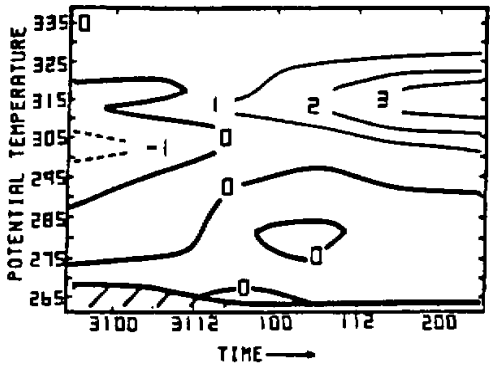

Fig. 23. Time variation of areally integrated eddy angular momentum transport (10^{18} kg m^2 s^{-2}) for the 7.5° radius for the Alberta cyclone from 0000 UTC 31 March to 0000 UTC 31 March to 0000 UTC 2 April 1971 with negative value for outward transport (Johnson et al., 1986).

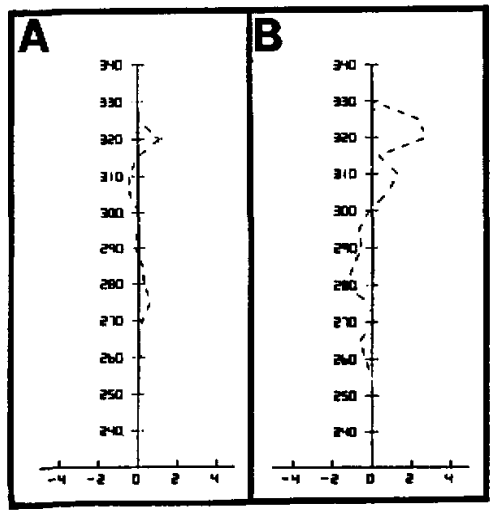

Fig. 24. Vertical profile of simulated azimuthally-averaged mass-weighted radial motion (m s^{-1} outflow positive) forced by horizontal eddy mode for the radius of 7.5° within the Alberta cyclone at (a) 0000 UTC 31 March and (b) 0000 UTC 2 April 1971.

baroclinic zone leads to the formation of an S-shaped upper-level-wind pattern (solid lines in Fig. 25b). This S-shaped upper-level-wind pattern at 310 K at 0000 UTC 2 April favors the inward eddy angular momentum transport (positive horizontal eddy mode at 310 K in

Fig. 23). Corresponding to the positive horizontal eddy mode, the radial motion around 310 K is outward at 0000 UTC 2 April (Fig. 24b).

(v) *The effect of frictional torque*

The frictional torque is calculated with the drag coefficient C_g^2 equal to 0.9×10^{-3} for all time periods. The results of this calculation (Fig. 59 in Yuan, 1994) show that the magnitudes of the radial motion forced by frictional torque intensify during the moist development. This is consistent with the time variation of frictional torque estimated in the previous diagnostic study of the Alberta cyclone (Fig. 6b in Johnson et al., 1976).

2.2.4 *Summary*

Two phases of development in the life cycle of the Alberta cyclone of March 30 – April 2, 1971 (Johnson et al., 1976; Katzfey, 1978; 1983) have been confirmed and simulated through the present numerical study. The first phase is called the leeside dry baroclinic development characterized by inward (outward) mass and angular momentum transport in higher (lower)

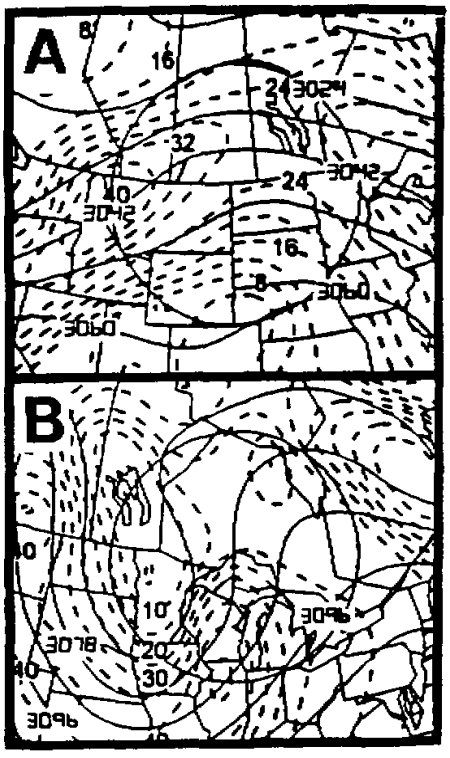

Fig. 25. Contours of Montgomery stream function 10^2 m^2 s^{-2}, solid) and isotachs (m s^{-1}, dashed) for the Alberta cyclone on (a) 305 K at 0000 UTC 31 March and (b) 310 K at 0000 UTC 2 April 1971. The circle with the radius equivalent to 7.5° latitudinal arc represents the position of the quasi-Lagrangian storm volume.

value isentropic layers. The present study shows that the lateral mass and angular momentum transport in this dry stage is mainly forced by inertial torque followed by pressure torque. The spin-up of the Alberta cyclone occurrs due to the excess of the inward angular momentum transport in the higher value isentropic layers over the outward transport in the lower value isentropic layers, as well as due to the angular momentum transfer from higher to lower value isentropic layers across inclined isentropic surfaces (mainly associated with inertial torque). The second phase is called the moist baroclinic development characterized by inward (outward) mass and angular momentum transport in lower (higher) value isentropic layers. In this moist stage, the lateral mass and angular momentum transport is mainly forced by pressure and inertial torque. The occlusion results from the vertical redistribution of angular momentum by pressure torque, inertial torque, eddy mode and diabatic heating. The transition from dry to moist radial-vertical circulation is mainly due to the decrease of positive inertial torque in the lower value isentropic layers and intensification of positive pressure torque in the higher value isentropic layers and negative pressure torque in the lower value isentropic layers.

3. Summary and conclusions

In this series of study (Johnson and Yuan, 1998; Yuan and Johnson, 1998), a linear second order differential equation was derived for investigating the forcing of the azimuthally averaged mass-weighted radial motion (equivalent to net convergence / divergence) within asymmetric translating extratropical and tropical cyclones by torques and diabatic heating. This equation had been applied to simulate the azimuthally averaged mass-weighted radial motion within three extratropical cyclones (the Ohio cyclone of 25–27 January 1978 and the two lee-side cyclones in this study) and typhoon Nancy of 18–23 September 1979 (Yuan and Johnson, 1998; present paper).

The results from present and previous studies (Johnson et al., 1976; Katzfey, 1978, 1983; Hale, 1983; Johnson and Hill, 1987; Johnson and Yuan, 1998; Yuan and Johnson, 1998) show that common features of these four cyclones are that 1) the azimuthally-averaged mass-weighted radial-vertical mass circulation is responsible for the net export of mass and import of angular momentum and the vertical redistribution of mass and angular momentum needed for the cyclone development, 2) the inward (outward) branch of the azimuthally averaged mass-weighted radial-vertical circulation is forced by negative (positive) torques and upward (downward) branch by diabatic heating (cooling) and 3) a stronger radial-vertical circulation occurs in response to weaker hydrodynamic stability for given forcing.

As expected, differences exist within extratropical and tropical cyclones. For the three extratropical cyclones, the main internal processes for forcing the radial-vertical circulation are associated with pressure torque and horizontal eddy angular momentum transport. For typhoon Nancy, the main factors are associated with latent heat release and weak hydrodynamic stability.

Differences also exist within extratropical cyclones in their early stage of development. The Ohio cyclone which formed over the southern part of the United States under the influence of continental polar air masses and Maritime tropical air masses, was characterized by strong baroclinicity. The inward mass and angular momentum transport through the radial motion was mainly forced by negative pressure torque in the lower value isentropic layers of the troposphere and in the stratospheric isentropic layers. The outward mass and angular momentum transport was mainly forced by positive pressure torque in the higher value

isentropic layers of the troposphere. The vertical redistribution of mass and angular momentum was due to non-convective transfer caused by pressure stress acting on inclined isentropic surfaces combined with upward diabatic transport associated with latent heat release.

In contrast, the Alberta cyclone of 30 March–2 April 1971 (a leeside cyclone), was influenced by the asymmetric distribution of hydrostatic mass due to the effects of the Rocky mountains and the confluence of maritime polar air masses and continental tropical air masses in the early stage (a dry stage). The inward (outward) mass and angular momentum transport through the radial motion was mainly forced by negative (positive) inertial torque in higher (lower) value isentropic layers (a dry pattern). The vertical redistribution of mass and angular momentum was due to the non-convective transfer associated with inertial and pressure torques. The decrease of positive inertial torque in the lower value isentropic layers and the intensification of positive pressure torque in the higher value isentropic layers and negative pressure torque in the lower value isentropic layers led to the reversal of the radial–vertical circulation from the dry pattern to the moist pattern.

Although the Mediterranean cyclone of 4–6 March 1982 was also a leeside cyclone, pressure torque and positive horizontal eddy mode due to the deformation of thermal structure under the effects of topography as well as the relatively warm mediterranean sea were responsible for the forcing of the radial motions with inward (outward) mass and angular momentum transport in lower (higher) value isentropic layers (a moist pattern). The azimuthally-averaged mass-weighted radial motion was also characterized by increasing intensity with radius in the early stage. The vertical redistribution of angular momentum was due to the upward diabatic transport associated with latent heat release and the non-convective transfer from the lower to higher value isentropic layers across inclined isentropic surfaces due to the paired negative and positive pressure torque.

All three cyclones attained a similar structure in their latter stage. The radial-vertical circulations within these three extratropical cyclones were all characterized by moist pattern with inflow (outflow) in lower (higher) value isentropic layers. The latent heat release and frictional torque contributed to the common state of an axially symmetric vortex.

For typhoon Nancy, the radial–vertical circulation was characterized by the moist pattern throughout its life cycle. CISK (Charney and Eliassen, 1964), which emphasized the importance of interaction between the latent heat release within the eyewall and forced inflow within the PBL was the main mechanism for providing Nancy with moist static energy and angular momentum needed for the development and maintenance.

This series of numerical simulation shows that the simulated radial motions within these four cyclones agree quite well with the "observed" radial motions. The excellent agreement verifies the existence of a forced azimuthally–averaged mass–weighted radial–vertical circulation with its systematic transport of angular momentum and enthalpy for the maintenance of a balanced vortex. The results from this numerical study substantiate the applicability of Eliassen's perspective to study the forcing of the azimuthally–averaged mass–weighted radial–vertical circulation by torques and diabatic heating within translating extratropical and tropical cyclones, and demonstrate the capability of the linear diagnostic equation to identify the relatively important internal physical processes in the development of cyclones.

The authors would like to thank Mr. Todd Schaack and Professor Kim Van Scoy for their scientific and editorial contributions. This research was sponsored by NASA Grant NAG5-81.

REFERENCES

Charney, J. G., and A. Eliassen, 1964: On the growth of the hurricane depression. *J. Atmos. Sci.*, **21**, 68–75.

Cressman, G. P., 1959: An operational objective analysis system. *Mon. Wea. Rev.*, **87**, 367–374.

Czarnetzki A. C., and D. R. Johnson, 1995: The role of terrain and pressure stresses in Rocky Mountain lee cyclones. *Mon. Wea. Rev.*, **124**, 553–570.

Eliassen, A., 1951: Slow thermally or frictionally controlled meridional circulation in a circular vortex. *Astrophysica Norvebica*, **5**, 19–60.

Garratt, J. R., 1977: Review of drag coefficients over ocean and continents. *Mon. Wea. Rev.*, **105**, 915–929.

Hale, R., 1983: Mass and angular momentum diagnostics of the intense Ohio Valley extratropical cyclone of 25–27 January 1978. M. S. Thesis, University of Wisconsin–Madison, 96 pp.

Hill, D. K., 1986: Quasi–Lagrangian mass and angular momentum diagnostics of the ALPEX lee cyclone of 4–6 March, 1982. M. S. Thesis, University of Wisconsin–Madison, 93 pp.

Holderback, C. S., 1982: *The moisture distribution of an Alberta cyclone*. M.S. Thesis, University of Wisconsin–Madison, 65 pp.

Johnson, D. R., and W. K. Downey, 1975a: Azimuthally averaged transport and budget equations for storms: Quasi–Lagrangian diagnostics 1. *Mon. Wea. Rev.*, **103**, 967–979.

Johnson, D. R., and W. K. Downey, 1975b: The absolute angular momentum of storms: Quasi–Lagrangian diagnostics 2. *Mon. Wea. Rev.*, **103**, 1063–1077.

Johnson, D. R., and Z. Yuan, 1998: On the forcing of the meridional circulation within cyclones, Part 1: Concepts and equations, Submitted.

----, C. H. Wash, and R. A. Peterson, 1976: The mass and absolute angular momentum budgets of the Alberta cyclone of 30 March–2 April 1971. *Sixth conference on weather forecasting and analysis, May 10–13, 1976, Albany, Massachusetts*, **02108**, 350–356.

----, and D. K. Hill, 1987: Quasi–Lagrangian diagnostic of a Mediterranean cyclone: Isentropic results. *Meteor. Atmos. Phys.*, **36**, 118–140.

----, 1981: The extratropical cyclone and its interaction with larger and smaller scales: Seminar presented at New Zealand Meteor. Service, Wellington, New Zealand, November 1981; and Seminar presented at Bureau Meteor., Melbourne, Australia, November 1981.

----, 1984: Leeside extratropical cyclone development and the relation of topography to acceleration of circulation. *Proceeding of the International Symposium on Tibetan Plateau and Mountain Meteorology*, Beijing, China, March 20–24, 1984, Science Press, Beijing and AMS, Boston, 435–470.

----, 1988: The extratropical cyclones, angular momentum and nonlinearity advanced study program of the National Center for Atmospheric Research, 1–7.

Katzfey, J., 1978: A diagnostic study of the vertical redistribution of angular momentum in isentropic coordinates by pressure torques. M. S. Thesis, University of Wisconsin–Madison, 118 pp.

Katzfey, J., 1983: On the role of the baroclinic structure in extratropical cyclone development. Ph. D. Thesis, University of Wisconsin–Madison, 265 pp.

Lorenz, E. N., 1955: Generation of available potential energy and the intensity of the general circulation. *In "Large Scale Synoptic Processes"* (J. Bjerknes, proj. dir.), Final Rep., 1957, Contract AF 19(604)–1286 Dept. Meteor., Univ. of California, Los Angeles.

Palmen, E., and C. W. Newton, 1969: *Atmospheric Circulation Systems. International Geophysics Series*. Academic Press, New York and London, **13**, 471–560.

Petterssen, S., 1956: *Weather Analysis and Forecasting* 2nd ed., Vol. I, McGraw–Hill, New York, 428 pp.

Rosinski, J., 1983: Mass and angular momentum diagnostics of hurricane Agnes during its transition to an extratropical cyclone. M.S. Thesis, University of Wisconsin–Madison, 67 pp.

Schneider, R., 1986: Quasi–Lagrangian diagostics of the 9–14 April 1979 Great Plains extratropical cyclones and subsynoptic scales. M. S. Thesis, University of Wisconsin–Madison, 152 pp.

Wash, C. H., 1978: Diagnostics of observed and numerically simulated extratropical cyclones. Ph. D. thesis, University of Wisconsin-Madison, 191 pp.

Whittaker, L. M., and L. H. Horn, 1982: Atlas of Northern Hemisphere extratropical cyclone activity 1958-1977, Department of Meteorology, University of Wisconsin-Madison, 65 pp.

Yuan, Z., 1994: The role of the diabatic heating, torques and stability in forcing the meridional circulation within cyclones. Ph. D. thesis, University of Wisconsin Madison, 198 pp.

Yuan, Z., and D. R. Johnson, 1998: The role of diabatic heating and stabilities in forcing the meridional circulation within cyclones, Part 2: Case study of extratropical and tropical cyclones, Submitted.